Chaotic motion on Hamiltonian tori

1993 J. Phys. A: Math. Gen. 26 261

(http://iopscience.iop.org/0305-4470/26/2/014)

J. Phys. A: Math. Gen. 26 (1993) 261–280. Printed in the UK

Chaotic motion on Hamiltonian tori

A von Kempis and H Lustfeld

Forschungszentrum Jülich (KFA), Postfach 1913, D-W-5170 Jülich, Federal Republic of Germany

Received 18 March 1992, in final form 27 July 1992

Abstract. KAM tori are well known to be that (finite!) part of phase space in which the motion of a weakly perturbed classical Hamiltonian system remains integrable. Moreover, they are barriers in the phase space of systems with two degrees of freedom. We show that certain Hamiltonian systems contain invariant *non-regular tori* with compressible flow. Using as an example an electron moving in electromagnetic fields which are periodic in space we demonstrate: (i) that strange attractors (and repellers) of well known autonomous or (quasi-)periodically time-driven systems may occur on such *strange tori*; (ii) that one may find *barriers* consisting of non-regular Hamiltonian tori in systems with any number of degrees of freedom (the flow on such barriers is non-chaotic, though); and (iii) that certain KAM tori transform into non-regular tori—rather than breaking up—when the perturbation becomes strong.

1. Introduction

In near-integrable Hamiltonian systems, integrable motion survives on so-called KAM tori [1–3]. Transforming to appropriate action-angle variables the equations of motion on a KAM torus situated at $\boldsymbol{I} = \boldsymbol{I}_0$ in action space can be cast into the form

$$\dot{\boldsymbol{I}} = \boldsymbol{0} \qquad \text{and} \qquad \dot{\boldsymbol{\Phi}} = \boldsymbol{\Omega}(\boldsymbol{I}_0) \qquad \text{at } \boldsymbol{I} = \boldsymbol{I}_0. \tag{1.1}$$

The motion on a KAM torus is universal in the sense that it depends on the frequency vector $\boldsymbol{\Omega}(\boldsymbol{I}_0)$ only and *not* on any detail of the nearly integrable system. In the neighbourhood of such a KAM torus the $\boldsymbol{\Phi}$-dependent term of the Hamiltonian (provided that the latter depends analytically on $\boldsymbol{I}$ and $\boldsymbol{\Phi}$) must be at least quadratic in $\boldsymbol{I} - \boldsymbol{I}_0$:

$$H = H_0(\boldsymbol{I}) + \varepsilon \sum_{\nu,\mu=1}^{N} (I_\nu - I_{0\nu}) h_{1\nu,\mu}(\boldsymbol{I}, \boldsymbol{\Phi})(I_\mu - I_{0\mu}). \tag{1.2}$$

Here ε is a small parameter indicating the weak non-integrability of the system.

Let us consider Hamiltonians which are only *linear* in $\boldsymbol{I} - \boldsymbol{I}_0$:

$$H = H_0(\boldsymbol{I}) + \eta(\boldsymbol{I} - \boldsymbol{I}_0) \cdot \boldsymbol{G}(\boldsymbol{I}, \boldsymbol{\Phi}). \tag{1.3}$$

0305-4470/93/020261+20$07.50

The parameter η need not be small. Clearly an invariant torus exists at $\boldsymbol{I} = \boldsymbol{I}_0$†. More general analytic Hamiltonians containing invariant tori which need not be KAM tori can be found by replacing the term $\boldsymbol{I} - \boldsymbol{I}_0$ in (1.3) with a vector field $\boldsymbol{F}$:

$$H = H_0(\boldsymbol{I}) + \eta \boldsymbol{F}(\boldsymbol{I}) \cdot \boldsymbol{G}(\boldsymbol{I}, \boldsymbol{\Phi})$$
$$\boldsymbol{F}(\boldsymbol{I}_*) = \boldsymbol{0} \qquad \text{for } \boldsymbol{I}_* \in M_n \qquad \dim M_n = n \leqslant N - 1 \tag{1.4}$$

where M_n is an n-dimensional manifold in action space. Hamiltonians of the form (1.3) are contained in (1.4) for $n = 0$. For $n > 0$ one finds an invariant torus for every action value $\boldsymbol{I}_*$ on the manifold M_n. Such tori are therefore not isolated in phase space: their union forms an invariant manifold with dimension $D_n = N + n \leqslant 2N - 1$ (note that for $D_n = 2N - 1$ these tori form a barrier in phase space, cf section 4.2). The equations of motion on such a torus situated at $\boldsymbol{I} = \boldsymbol{I}_* \in M_n$ read

$$\dot{\boldsymbol{\Phi}} = \boldsymbol{\omega}_0(\boldsymbol{I}_*) + \eta \frac{\partial \boldsymbol{F}}{\partial \boldsymbol{I}_*} \boldsymbol{G}(\boldsymbol{I}_*, \boldsymbol{\Phi}) \qquad \text{where } \boldsymbol{\omega}_0 = \frac{\partial H_0}{\partial \boldsymbol{I}}. \tag{1.5}$$

For small η the probability is finite that these tori will again be KAM tori—which means that, applying KAM perturbation theory, one may find a time-independent canonical transformation of the angles alone removing the term of the Hamiltonian (1.4) which is linear in $\boldsymbol{I} - \boldsymbol{I}_0$ [4, 5] (two simple explicit examples are given [6]; cf also [7]). Even for small η the procedure does not converge in the neighbourhood of resonances which means that (generically) it will not converge in any η-interval. The points on the η-axis where such a transformation exists form a set of finite measure, though, and the latter tends to 1 with $\eta \to 0$. For large η the strength of the perturbation will generically destroy all KAM tori, and the same is true in the strong-coupling limit $H_0 \to 0$ ($\Rightarrow \boldsymbol{\omega}_0(\boldsymbol{I}_*) \to \boldsymbol{0}$). We call these tori which are not of the KAM type *non-regular tori*. In contrast to the *regular tori* in integrable and nearly integrable systems (the latter are the KAM tori) they clearly cannot be classified by just one frequency vector $\boldsymbol{\Omega}$.

Whereas the equations of motion (1.1) on KAM tori are trivially integrable the motion on these non-regular tori is of a different type, as may already have been guessed from the equations of motion (1.5). These show that the motion on the invariant tori of systems of the type (1.4) are usually dissipative because the divergence rate of the flow *on* these tori, i.e.

$$\nabla_{\boldsymbol{\Phi}} \cdot \dot{\boldsymbol{\Phi}} = \eta \nabla_{\boldsymbol{\Phi}} \cdot \left(\frac{\partial \boldsymbol{F}}{\partial \boldsymbol{I}_*} \boldsymbol{G}(\boldsymbol{I}_*, \boldsymbol{\Phi}) \right) \tag{1.6}$$

needs not vanish‡ (note that the vector function $\boldsymbol{G}(\boldsymbol{I}, \boldsymbol{\Phi})$ is only required to be 2π-periodic in the angles $\boldsymbol{\Phi}$). Therefore, attractors may occur in the flow on non-regular

† A manifold in phase space is called an *invariant* manifold if the direction of the flow (i.e. of the phase space velocity) is everywhere tangential to it.

‡ Since the ensemble density $\rho_{\boldsymbol{x}}$ in the phase-space of the variables $\boldsymbol{x}$ is subject to the continuity equation $\dot{\rho}_{\boldsymbol{x}} + \rho_{\boldsymbol{x}} \nabla_{\boldsymbol{x}} \cdot \dot{\boldsymbol{x}} = 0$ one has $\nabla_{\boldsymbol{x}} \cdot \dot{\boldsymbol{x}} = \dot{V}_{\boldsymbol{x}} / V_{\boldsymbol{x}}$ where $V_{\boldsymbol{x}} = 1/\rho_{\boldsymbol{x}}$ is the specific phase-space volume. Thus, the local divergence rate equals the relative change of the specific phase space volume per unit time. In Hamiltonian systems $\boldsymbol{x} = (\boldsymbol{I}, \boldsymbol{\Phi})$, and thus $\nabla_{\boldsymbol{x}} \cdot \dot{\boldsymbol{x}} = \nabla_{\boldsymbol{\Phi}} \cdot \dot{\boldsymbol{\Phi}} + \nabla_{\boldsymbol{I}} \cdot \dot{\boldsymbol{I}} = \nabla_{\boldsymbol{\Phi}} \cdot (\nabla_{\boldsymbol{I}} H) + \nabla_{\boldsymbol{I}} \cdot (-\nabla_{\boldsymbol{\Phi}} H) = 0$ which implies $\dot{\rho}_{\boldsymbol{x}} = 0$ (Liouville's law). Analogously, on an invariant N-torus situated at $\boldsymbol{I} = \boldsymbol{I}_*$ in action space one finds that $\nabla_{\boldsymbol{\Phi}} \cdot \dot{\boldsymbol{\Phi}} \,|_{\boldsymbol{I}_*} = \dot{V}_{\boldsymbol{\Phi}} / V_{\boldsymbol{\Phi}}$ where $V_{\boldsymbol{\Phi}} = 1/\rho_{\boldsymbol{\Phi}}$ is the N-dimensional specific *torus* volume (whereas $\dim V_{\boldsymbol{x}} = 2N$ in general).

tori. This is no contradiction to Liouville's theorem concerning the conservation of the $2N$-dimensional phase-space volume since it vanishes identically on a given N-torus, and the same holds for all other Poincaré invariants. Thus, these conservation laws do *not* forbid dissipative or antidissipative motion on invariant tori. On KAM tori the system still 'feels' the presence of the N commuting conserved quantities of the unperturbed system, whereas on non-regular tori the situation may be compared with a system having N non-commuting conserved quantities of the motion. In such systems the flow is restricted to an N-dimensional manifold but on this manifold chaotic motion is not usually excluded. Dissipative motion on invariant tori must naturally be compensated for by antidissipative motion in their neighbourhood (see later). Furthermore, the flow on tori cannot be dissipative everywhere since the mean local divergence rate vanishes due to the 2π-periodicity of the equations of motion:

$$\oint \nabla_{\Phi} \cdot \dot{\Phi}(I_*, \Phi)\, \mathrm{d}^N \Phi = 0. \tag{1.7}$$

This is in contrast to conventional dissipative systems where the local divergence rate is usually negative-definite. For instance, in the well known systems of Lorenz [8] or Duffing (cf section 4.1) the value of the divergence rate $\nabla_x \cdot \dot{x}$ is uniform in phase space.

Some aspects of the motion on tori have been discussed in recent studies in the context of dissipative systems. Grebogi and Battelino [9–11] demonstrated numerically that quasiperiodic motion does generically persist on invariant N-tori ($N = 3$ or 4) for finite perturbations while Baesens *et al* [12] concentrated on the study of resonances and global bifurcations in systems of three weakly coupled oscillators. In these studies the continuous dynamics is always reduced to discrete maps by analysing a Poincaré or return map of the motion on the torus. This is only possible if at least one integer linear combination of the angle variables advances monotonically in time. As we will see, this excludes Hamiltonian systems with *isolated* invariant tori (which are implicitly considered in these studies) in the range of large perturbation ($\eta \gtrsim 1$) or strong coupling ($H_0 \to 0$) which we will investigate later—simply because then there are (generically) no angles, or integer linear combinations of angles, advancing monotonically for indefinite time. In the long-time limit the motion is thus confined to relatively small parts of the torus where the local divergence rate is negative-definite and—after a transient phase—the trajectories converge towards attractors which (as we will show) may also be strange ones†. Since the divergence rate vanishes when averaged over the whole torus it is no surprise to find (strange) attractors also in the study of the time-reversed flow. These attractors are repellers of the non-time-reversed flow. We call non-regular tori containing strange attractors (or repellers) *strange tori* for short.

In this study we always restrict our attention to the motion *on* non-regular tori. As the flow in phase space as a whole cannot be compressible, dissipative motion on such tori has naturally to be compensated for by antidissipative motion in their neighbourhood, i.e. in action space, and *vice versa*. For sufficiently large perturbation strength—$\eta \gtrsim 1$—nearly all trajectories on these tori tend towards attractors in the long-time limit. Therefore, for nearly all initial conditions non-regular tori are strongly repulsive in action space if η is sufficiently large. Trajectories starting near non-regular

† In the previously mentioned paper [12] Baesens *et al* describe another form of chaotic motion on invariant tori, namely chaotic variations of the winding numbers, which they call 'toroidal chaos'.

tori can approach such a torus only during the transient phase, provided the initial conditions in the angles are situated near a repeller, or if the initial conditions in the angles are situated on a repeller (then exponentially fast for indefinite time). Some explicit examples have been worked out in [6] (see also [7]).

The paper is organized as follows. In section 2 we demonstrate that Hamiltonians of the form (1.3) and (1.4) do occur in physics, namely for a *single* charged particle (e.g. an electron) moving in certain electromagnetic fields which are periodic in space. Section 3 is devoted to the study of the flow on isolated strange tori containing well known strange attractors of autonomous systems, such as those studied by Lorenz [8] or Rössler [13]. Non-isolated non-regular Hamiltonian tori are inspected in section 4. We find that: (i) well known attractors of periodically or quasiperiodically driven systems occur on such tori, e.g. those found in Duffing's oscillator system [14, 15]; (ii) the flow on non-isolated N-tori forming a barrier cannot be chaotic (but may contain strange non-chaotic attractors [16] if $N \geqslant 3$); and (iii) periodic motion may be impossible if $N \geqslant 3$. Conclusions are given in section 5.

2. An electron moving on non-regular Hamiltonian tori

Before studying the properties of the flow on non-regular Hamiltonian tori in more detail let us show that such tori, both isolated and non-isolated ones, may indeed occur in physical systems, namely for an electron moving in certain stationary or (quasi-) periodically time-dependent electromagnetic fields which are periodic in space.

The Hamiltonian of a non-relativistic 'classical electron' (without spin) moving in an electromagnetic field reads (in MKS units)

$$\mathcal{H} = \frac{1}{2m_{\mathrm{e}}}(\boldsymbol{P} - e\boldsymbol{A}(\boldsymbol{r},t))^2 + e\phi(\boldsymbol{r},t) \tag{2.1}$$

where $\boldsymbol{A}$ and ϕ are the magnetic vector potential and the electric potential, respectively, $e = -e_0$ is the charge of the electron, and $\boldsymbol{P} = m_{\mathrm{e}}\dot{\boldsymbol{r}} + e\boldsymbol{A}(\boldsymbol{r},t)$ is its canonical momentum. If one can find a constant $\boldsymbol{P}_0$ such that—for some gauge—the electric potential fulfils the condition

$$\phi(\boldsymbol{r},t) = \frac{\boldsymbol{P}_0 \cdot \boldsymbol{A}(\boldsymbol{r},t)}{m_{\mathrm{e}}} - \frac{e}{2m_{\mathrm{e}}}\boldsymbol{A}^2(\boldsymbol{r},t) \tag{2.2}$$

the Hamiltonian (2.1) takes the form

$$\mathcal{H} = \frac{\boldsymbol{P}^2}{2m_{\mathrm{e}}} - \frac{e}{m_{\mathrm{e}}}(\boldsymbol{P} - \boldsymbol{P}_0) \cdot \boldsymbol{A}(\boldsymbol{r},t). \tag{2.3}$$

For vector potentials $\boldsymbol{A}$ which are periodic in space, i.e. which fulfil

$$\boldsymbol{A}(\boldsymbol{r} + \boldsymbol{r}_i) = \boldsymbol{A}(\boldsymbol{r}) \qquad i = 1,2,3 \tag{2.4}$$

for three linearly independent vectors $\boldsymbol{r}_{i=1,2,3}$, the Hamiltonian (2.3) may be written either in the form (1.3) or in the form (1.4). Because of the periodicity properties of the electromagnetic potentials† one can always find a linear transformation to

† These imply a corresponding space periodicity of the electromagnetic fields and (via the inhomogeneous Maxwell equations) of the charge and current densities producing these fields.

action-angle coordinates. For magnetic vector potentials whose space periodicity is characterized by cubic basis cells, i.e.

$$r_1 = (x_0, 0, 0) \qquad r_2 = (0, y_0, 0) \qquad r_3 = (0, 0, z_0) \tag{2.5}$$

one has, e.g.,

$$\boldsymbol{\Phi} = 2\pi \left(\frac{x}{x_0}, \frac{y}{y_0}, \frac{z}{z_0} \right) \qquad \text{and} \qquad \boldsymbol{I} = \frac{1}{2\pi}(x_0 P_x,\ y_0 P_y,\ z_0 P_z) \tag{2.6}$$

and the Hamiltonian (2.3) is transformed to

$$H = \sum_{i=1}^{3} \int \omega_0(I_i)\, \mathrm{d}I_i + \eta(\boldsymbol{I} - \boldsymbol{I}_0) \cdot \boldsymbol{G}(\boldsymbol{\Phi}, t)$$

where

$$\boldsymbol{\omega}_0(\boldsymbol{I}) = \frac{4\pi^2}{m_e} \left(\frac{I_1}{x_0^2}, \frac{I_2}{y_0^2}, \frac{I_3}{z_0^2} \right) \qquad \text{and} \qquad \boldsymbol{G}(\boldsymbol{\Phi}, t) = -\frac{e}{m_e} \frac{2\pi}{\eta} \left(\frac{A_x}{x_0}, \frac{A_y}{y_0}, \frac{A_z}{z_0} \right). \tag{2.7}$$

The Hamiltonian (2.7) is of the type (1.3) if $\boldsymbol{A}$ has three linearly independent components whereas it is of the type (1.4) if $\boldsymbol{A}$ has $m < 3$ linearly independent components, i.e.

$$\boldsymbol{A} = \sum_{j=1}^{m \leqslant 2} c_j \tilde{A}_j \qquad \text{with } \tilde{A}_j(\boldsymbol{r} + \boldsymbol{r}_{i=1,2,3}) = \tilde{A}_j(\boldsymbol{r}) \qquad j \leqslant m < 3. \tag{2.8}$$

There is an invariant torus for action vectors satisfying the m conditions

$$\tilde{c}_{j1} I_{*,1} + \tilde{c}_{j2} I_{*,2} + \tilde{c}_{j3} I_{*,3} = \tilde{c}_j \cdot \boldsymbol{I}_0 \qquad \text{where } \tilde{c}_j = \left(\frac{c_1}{x_0}, \frac{c_2}{y_0}, \frac{c_3}{z_0} \right) \qquad j \leqslant m < 3. \tag{2.9}$$

For $m = 1$ this condition specifies a plane M_2 that divides the three-dimensional action space into two parts which cannot be joined by trajectories. Thus, the invariant tori with actions $\boldsymbol{I}_* \in M_2$ form a barrier in phase space. For $m = 2$ the two linearly independent conditions specify a straight line M_1. Therefore, the invariant tori with actions $\boldsymbol{I}_* \in M_1$ form a four-dimensional planar area in the six-dimensional phase space.

It should be emphasized that the Hamiltonian (2.1) is gauge-invariant, i.e. a canonical transformation exists which leaves it form invariant with respect to a gauge-transformation of the electromagnetic potentials [6]. Clearly, this is not the case for the Hamiltonians (2.3) and (2.7) since the condition (2.2) is not gauge-invariant. This does not mean that the presence of non-regular tori depends on the choice of the gauge. Rather, it depends on the choice of the electric (or: electromagnetic) field(s).

For later use (namely in section 4.1) we note that non-regular Hamiltonian tori may occur in the non-relativistic motion of an electron in time-dependent fields as well, and also when the motion is restricted to only one or two spatial degrees of freedom. With regard to this latter case let, e.g., $A_z = 0$. Then $\dot{\Phi}_3 = (2\pi/z_0)\dot{z} = \omega_{0,3}(\boldsymbol{I}_*) = \text{constant}$ for $\boldsymbol{I}_* \in M_{3-m}$ which implies $\ddot{z} = 0$ whereas in the general case, i.e. if the electric potential does not fulfil the condition (2.2), or beyond the invariant tori considered here, $\ddot{z} = 0$ implies $A_z = 0$ *and* $\partial A_x/\partial z = \partial A_y/\partial z = 0$.

3. Isolated non-regular Hamiltonian tori

We proceed to show that, for any given attractor of a dynamical system which can be described by autonomous ordinary differential equations, one can easily find a Hamiltonian system containing an isolated invariant non-regular torus where this attractor occurs, provided the extension of the attractor is finite. Thus, if the dissipative system—written in the form of first-order differential equations—consists of no more than three equations one may specify electromagnetic fields such that a non-relativistic electron with appropriate momentum moves on a non-regular torus containing any such attractor. As an example we consider a torus containing the strange attractor of Rössler's system [13]. In section 3.2 we investigate certain symmetry properties of the flow on these somewhat special non-regular tori related to fixed points or time-reversal, respectively. In section 3.3 we explain the method used to find all attractors on isolated non-regular tori and give a short account of our results concerning the strange 'Rössler torus' which contains several, and in many cases coexisting, attractors, namely two point attractors and two periodic attractors (limit cycles) where the latter transform into strange attractors via sequences of period-doublings when η is decreased or, in the case of Rössler's strange attractor, increased. In addition, every attractor is connected to a structurally identical repeller by a one-to-one transformation.

3.1. *Attractors of autonomous systems on non-regular tori*

The procedure is straightforward. Take any (nonlinear) autonomous system of ordinary differential equations with M control parameters. If necessary transform it into a system of first order $\dot{\boldsymbol{x}} = \boldsymbol{f}(\boldsymbol{x}; p_1, \ldots, p_M)$ or, in scalar notation,

$$\dot{x}_i = f_i(x_{j=1,\ldots,N}; p_{r=1,\ldots,M}) \qquad i = 1, \ldots, N. \tag{3.1}$$

If it contains an attractor of finite size in the N-dimensional phase space of the variables $\boldsymbol{x}$ transform (rescale and/or shift) these variables—if necessary—such that the attractor is situated near the origin. Then replace

$$f_i(x_j; p_r) \to \tilde{f}_i(x_j; p_r) = f_i\left(\alpha \sin \frac{x_j}{\alpha}; p_r\right) \tag{3.2}$$

where α is a new parameter. In this way one creates the modified system

$$\dot{x}_i = f_i\left(\alpha \sin \frac{x_j}{\alpha}; p_r\right). \tag{3.3}$$

It is clear that due to

$$\lim_{x/\alpha \to 0} \alpha \sin \frac{x}{\alpha} = x \tag{3.4}$$

the modified system (3.3) tends to the original one (3.1) for $\boldsymbol{x}/\alpha \to \boldsymbol{0}$. Since the right-hand side of (3.3) is 2π-periodic in the new variables $\boldsymbol{\Phi} = \boldsymbol{x}/\alpha$, substitution of variables leads to

$$\dot{\Phi}_i = \frac{1}{\alpha} f_i(\alpha \sin \Phi_j; p_r). \tag{3.5}$$

Let us identify the right-hand side of this system with the vector field $\boldsymbol{G}(\boldsymbol{\Phi})$:

$$\boldsymbol{G}(\boldsymbol{\Phi}) \equiv \frac{1}{\alpha}\boldsymbol{f}(\alpha \sin \Phi_1, \ldots, \alpha \sin \Phi_N; p_1, \ldots, p_M). \tag{3.6}$$

This vector field is 2π-periodic in the variables $\boldsymbol{\Phi}$ (as required). If we insert it into the equations of motion (1.5) for $n = 0$ we get the system

$$\dot{\boldsymbol{\Phi}} = \boldsymbol{\omega}_0(\boldsymbol{I}_0) + \frac{\eta}{\alpha}\boldsymbol{f}(\alpha \sin \Phi_1, \ldots, \alpha \sin \Phi_N; p_1, \ldots, p_M) \tag{3.7}$$

on the torus situated at $\boldsymbol{I} = \boldsymbol{I}_0$. Denoting by a prime the derivative with respect to a scaled time $\tau = \eta t$ we arrive at

$$\boldsymbol{\Phi}' = \frac{\boldsymbol{\omega}_0(\boldsymbol{I}_0)}{\eta} + \frac{1}{\alpha}\boldsymbol{f}(\alpha \sin \Phi_1, \ldots, \alpha \sin \Phi_N; p_1, \ldots, p_M). \tag{3.8}$$

Starting from a Hamiltonian of the form

$$H = \frac{H_0(\boldsymbol{I})}{\eta} + (\boldsymbol{I} - \boldsymbol{I}_0) \cdot \boldsymbol{G}(\boldsymbol{I}, \boldsymbol{\Phi}) \tag{3.9}$$

rather than from one of the form (1.3) and proceeding as before one arrives at an equation of motion of the same form as (3.8) but with the derivative taken with respect to the unscaled time variable t:

$$\dot{\boldsymbol{\Phi}} = \frac{\boldsymbol{\omega}_0(\boldsymbol{I}_0)}{\eta} + \frac{1}{\alpha}\boldsymbol{f}(\alpha \sin \Phi_1, \ldots, \alpha \sin \Phi_N; p_1, \ldots, p_M). \tag{3.10}$$

In the limit

$$\boldsymbol{\Phi} = \frac{\boldsymbol{x}}{\alpha} \to \boldsymbol{0} \qquad \text{and} \qquad \eta \to \infty \tag{3.11}$$

the system (3.8) tends to $\boldsymbol{x}' = \boldsymbol{f}(\boldsymbol{x}; p_1, \ldots, p_M)$, i.e. to the original system but with respect to scaled time, and the system (3.10) tends to the original system (3.1). In this limit an attractor of the original system situated near the origin will therefore also show up in the earlier systems of equations of motion (3.8) or (3.10), respectively†, in the neighbourhood of the origin and its equivalent locations, i.e. near

$$\boldsymbol{\Phi} = 2\pi \boldsymbol{l} \qquad \boldsymbol{l} \in \mathbb{Z}^N. \tag{3.12}$$

Note that the limiting case $\eta = \infty$ can be realized (alternatively) by the parameter values

$$\boldsymbol{\omega}_0(\boldsymbol{I}_0) = \boldsymbol{0} \qquad \text{and} \qquad \eta = 1 \tag{3.13}$$

† There is a subtlety in the limit (3.11) on which we would like to comment: keeping the parameters $\{p_r\}$ fixed the Lyapunov exponents converge to those of the original attractor in the limit (3.11) if the attractor is structurally stable. If it is not we can find parameters $\{p_r\}$ depending on α and η such that the Lyapunov exponents *and* the $\{p_r\}$ converge to those of the original attractor in this limit.

i.e. by starting with the Hamiltonian

$$H = (I - I_0) \cdot G(\Phi) \tag{3.14}$$

to which we will refer below as the 'perturbing system' of the Hamiltonian (1.3).

Clearly *all* finite-sized attractors occurring in autonomous systems of differential equations also occur on isolated invariant tori of Hamiltonian systems which may be specified by the procedure described in this section. Yet, this statement is rigorous only in the limit $\alpha \to \infty$. For finite values of the scaling parameter α the behaviour near the origin—and its equivalent locations—does not change much if α is large, cf the following example. We apply the previously described procedure to Rössler's system [13]

$$\begin{aligned} \dot{x} &= -y - z \\ \dot{y} &= x + ay \\ \dot{z} &= b + z(x - c) \end{aligned} \tag{3.15}$$

where a, b, c are the control parameters. Rössler [13] used

$$a = 0.2 \qquad b = 0.2 \qquad c = 5.7. \tag{3.16}$$

If we identify system (3.15) with system (3.1) and insert it into equation (3.8) we find the following equations of motion on the torus situated at $I = I_0$:

$$\begin{aligned} \Phi_1' &= \frac{\omega_{0,1}}{\eta} - \sin\Phi_2 - \sin\Phi_3 \\ \Phi_2' &= \frac{\omega_{0,2}}{\eta} + \sin\Phi_1 + a\sin\Phi_2 \\ \Phi_3' &= \frac{\omega_{0,3}}{\eta} + \frac{b}{\alpha} + \alpha\sin\Phi_3\left\{\sin\Phi_1 - \frac{c}{\alpha}\right\}. \end{aligned} \tag{3.17}$$

As discussed in section 2 it is easy to specify electromagnetic potentials such that the motion of a non-relativistic electron with appropriate momentum proceeds on an invariant 3-torus with given equations of motion. In the present case the vector potential may easily be found by comparing the foregoing equations of motion with the equations of motion on the non-regular torus of Hamiltonian (2.7) and resubstituting for the angles from (2.6). The necessary electric potential is defined by (2.2). Beyond the 'Rössler torus' the frequency $\omega_0(P)$ depends linearly on the canonical momentum, cf section 2.

For sufficiently large values of α one expects to find an attractor near the origin which should be very similar to the strange attractor of Rössler's system (3.15) if $\omega_0(I_0) = 0$ and $\eta = 1$, which implies (as initial conditions) $m_e\dot{r} = -eA(r)$ or (alternatively) in the limit $\eta \to \infty$. Figure 1 shows this attractor—centred around an unstable fixed point—for $\alpha = 100$ and Rössler's control parameter values (3.16). The attractors are so similar that their plots look the same. For not too large α they can be distinguished, however, by computing their one-dimensional Lyapunov exponents with the algorithm of Wolf *et al* [17]. The definition of the Lyapunov exponents employed here is the more usual one—exponents relative to the base e—rather than

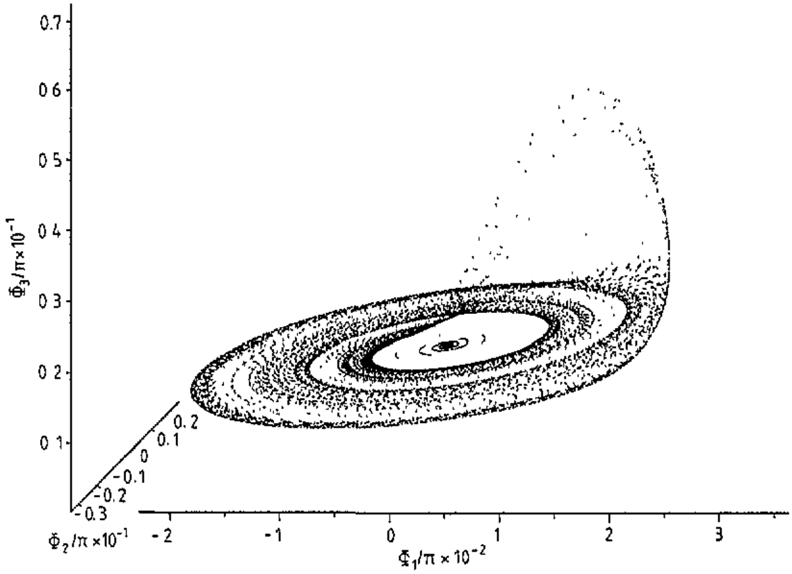

Figure 1. The 'Rössler-like' attractor on the 'Rössler torus', centred around an unstable fixed point; $\eta = \infty$ and $\alpha = 100$ (this value of α is used throughout).

the one used in [17] (exponents relative to the base 2). For the 'Rössler-like' attractor displayed in figure 1 one finds

$$\lambda_1 = 0.06 \qquad \lambda_2 = 0 \qquad \lambda_3 = -5.39 \tag{3.18}$$

while the original Rössler attractor is characterized by

$$\lambda_1 = 0.07 \qquad \lambda_2 = 0 \qquad \lambda_3 = -5.39 \tag{3.19}$$

which indicates a slightly more chaotic behaviour†.

3.2. Symmetry analysis of the flow

As discussed in the introduction, the motion far from the origin will greatly differ from the one near the origin in Hamiltonian systems of the form (1.3) or (3.9), respectively, since dissipative regions on tori have to be complemented by antidissipative ones. Much about this behaviour can be learned by exploiting the symmetry property of the sine function

$$\sin\varphi = \sin(\pi - \varphi). \tag{3.20}$$

Let us look first at the fixed points of the equations of motion (3.8) or (3.10), respectively, on strange tori. Assuming that at least one fixed point Φ_* does exist—and every fixed point of the original system (3.1) implies the existence of such a fixed point in the limit $\alpha \to \infty$ (and $\eta \to \infty$ or, alternatively, $\omega_0(I_0) = 0$ and $\eta = 1$)—the

† There is always a vanishing exponent related to the direction of the flow except for trajectories ending on a fixed point [18].

existence of $2^N - 1$ further and non-equivalent fixed points follows from this symmetry relation if

$$\Phi_{*,i} \neq \tfrac{1}{2}\pi + l\pi \qquad l \in \mathbb{Z} \qquad \text{for all } i = 1, \ldots, N \tag{3.21}$$

since then one has $\Phi_{*,i} \neq \pi - \Phi_{*,i}$ for all angles†. Using the notation

$$\Phi_i^{[0]} = \Phi_i \qquad \Phi_i^{[1]} = \pi - \Phi_i \tag{3.22}$$

any one of these 2^N fixed points may be characterized by a string of N bits $[n_1, \ldots, n_N]$ via

$$\mathbf{\Phi}_*^{[n_1,\ldots,n_N]} = (\Phi_{*,1}^{[n_1]}, \ldots, \Phi_{*,N}^{[n_N]}) \qquad \text{where } n_{i=1,\ldots,N} \in \{0;1\}. \tag{3.23}$$

Among them we denote by $[0,0,0]$ the fixed point next to the origin. Each fixed point $[n_1, \ldots, n_N]$ generates a lattice of equivalent fixed points with lattice constants 2π in every component.

Where fixed points of the motion on a strange torus exist one will naturally perform a linear stability analysis of the motion near them. Since the right-hand side of an equation of motion vanishes at a fixed point, expanding system (1.5) for $n = 0$ around $\mathbf{\Phi}_*$ leads to

$$\mathbf{\Phi}' \,|_{I_0} = \left.\frac{\partial G(I_0, \mathbf{\Phi})}{\partial \mathbf{\Phi}}\right|_{\mathbf{\Phi}_*} (\mathbf{\Phi} - \mathbf{\Phi}_*) + \cdots. \tag{3.24}$$

The eigenvalues of the matrix $\partial G / \partial \mathbf{\Phi}_* \,|_{I_0}$ characterize the flow near $\mathbf{\Phi}_*$ (if e.g. all eigenvalues are negative the fixed point is an attractor). For vector fields $G(\mathbf{\Phi})$ defined via (3.6) one has

$$\frac{\partial G_i}{\partial \Phi_{*,j}} = \frac{\partial G_i}{\partial \sin \Phi_{*,j}} \cos \Phi_{*,j}. \tag{3.25}$$

Therefore, any fixed point $[n_1, \ldots, n_N]$ has a *conjugated* partner $[\overline{n_1}, \ldots, \overline{n_N}]$ among the other $2^N - 1$ ones, namely

$$\overline{\mathbf{\Phi}}_*^{[\overline{n_1},\ldots,\overline{n_N}]} = (\pi - \Phi_{*,1}^{[n_1]}, \ldots, \pi - \Phi_{*,N}^{[n_N]}) \equiv \pi - \mathbf{\Phi}_*^{[n_1,\ldots,n_N]} \tag{3.26}$$

with the opposite eigenvalues since $\cos\varphi = -\cos(\pi - \varphi)$.

Comparing more generally the equations of motion of a point $\mathbf{\Phi}$ to those of the *conjugated* point

$$\overline{\mathbf{\Phi}} = (\pi - \Phi_1, \ldots, \pi - \Phi_N) \equiv \pi - \mathbf{\Phi} \tag{3.27}$$

we see that $\dot{\overline{\mathbf{\Phi}}} = -\dot{\mathbf{\Phi}}$. Furthermore, for vector fields $G(\mathbf{\Phi})$ defined via a relation of the form (3.6), the symmetry relation (3.20) of the sine function leads to $G(\overline{\mathbf{\Phi}}) = G(\mathbf{\Phi})$. Therefore, the equations of motion of a point $\mathbf{\Phi}$ are fully equivalent to the time-reversed equations of motion of the conjugated point $\overline{\mathbf{\Phi}}$. Stated more formally: if $\mathbf{\Phi}(t)$ solves the equations of motion then $\overline{\mathbf{\Phi}}(-t) = \pi - \mathbf{\Phi}(-t)$ is also a solution, and *vice versa* (since $\overline{\overline{\mathbf{\Phi}}} = \mathbf{\Phi}$). Any trajectory has thus a counterpart under time-reversal which is simply shifted and reflected with respect to the original one by the transformation (3.27). As a consequence all attractors also occur in the time-reversed flow, yet transformed via (3.27). Every attractor of the motion forward in time is thus matched by a repeller of the same type—cf the previous example of the fixed points.

† If condition (3.21) is violated for one angle there are only $2^{N-1} - 1$ further non-equivalent fixed points, etc.

3.3. Attractors and repellers on isolated strange tori

To obtain a more comprehensive picture of the motion on isolated strange tori it is useful to complement the symmetry considerations and the linear stability analysis of the foregoing section with numerical investigations. We are especially interested in finding *all* attractors on the torus, both for the torus of the 'perturbing system' (3.14) and for the corresponding tori at finite values of η. In the latter case we concentrate on the region of relatively large perturbations ($\eta \gtrsim 1$) or strong coupling (H_0 small), i.e. on invariant tori where the flow contains fixed points, since these have not yet been considered elsewhere (cf section 1).

Point attractors are found by solving the fixed point equations $\dot{\mathbf{\Phi}}\,|_{\Phi_*} = \mathbf{0}$ and performing a linear stability analysis of the motion near all fixed points (cf section 3.2). In order to find all non-point attractors we used the following procedure: Near each of the fixed points on the torus which are *not* point attractors $2N$ initial conditions were selected, pairwise displaced parallel to the N (perpendicular) axis on either side of each such fixed point, and the subsequent motion was tracked. The idea behind this procedure is to explore the unstable manifold(s) of all unstable fixed points since the stable manifolds of attractors do generically intersect the unstable manifolds of fixed points (this is true for point attractors and conjectured for others). Thus, exploring the unstable manifolds of all (unstable) fixed points should reveal all attractors. We used the method for studying the flow on two different isolated strange 3-tori, namely on the strange 'Rössler torus' (cf section 3.1) on the one hand and on the strange 'Lorenz torus' on the other (the latter is related to the Lorenz system [8] in the same way as is the 'Rössler torus' to Rössler's system [13]). It turned out that whenever an attractor was found it also attracted at least one of the trajectories in the sample thus defined. In order to find the corresponding repellers of the flow—i.e. the attractors of the time-reversed flow—it suffices to apply the transformation (3.27) to these attractors.

Let us briefly summarize the results of our numerical analysis [6] for the 'Rössler torus' (using the control parameters (3.16) taken by Rössler in [13]). As we have seen in section 3.1 the Lyapunov exponents depend only weakly on the scaling for $\alpha \gtrsim 100$, and the same is true for the eigenvalues of the linearized motion near fixed points. Therefore, the value $\alpha = 100$ is used throughout. The numerical value of the unpertubed frequencies ω_0 is of similar insignificance (and in the limiting case $\eta = \infty$ or in the 'perturbing system', respectively, it does not matter at all). We inserted $\omega_0 = (\sigma_g, \sigma_g^2, 1)$ where $\sigma_g = (\sqrt{5}-1)/2$ is the golden mean. Then the torus is a KAM torus in the limiting case $\eta = 0$. Still, for not too small values of η—especially in the range where fixed points exist—one finds qualitatively the same behaviour for any other choice of the frequencies ω_0.

For these parameters we find three types of attractors on the strange 'Rössler torus':

(i) For very large η-values there is a 'Rössler-like' attractor near the origin, centred around an unstable fixed point (cf section 3.1 and figure 1). Near $\eta = 1$ one finds a simple limit cycle in its place which goes through a sequence of period doublings when η is increased, cf figure 2. The attractor turns chaotic near $\eta \approx 170$. Periodic windows (e.g. of period three) are found at higher η-values. This interpretation of the transformation of the attractor with increasing η is confirmed by the fact that Crutchfield *et al* [19] have shown that by varying control parameter c in Rössler's system (3.15) one proceeds via a period-doubling sequence from a simple limit cycle to Rössler's strange attractor.

(ii) The positions of the fixed points may be calculated analytically by solving a quadratic equation for $\sin\Phi_{*,1}$. Therefore, one finds two sets of fixed points, each containing $2^3 = 8$ fixed points, cf section 3.2. The eigenvalues of the fixed points are found by solving the cubic characteristic equation related to the 3×3 matrix in (3.24). As long as the fixed points are real-valued (i.e. for $\eta \gtrsim 1$) each set of fixed points contains a point attractor. Note that real-valued fixed points exist only if α is not too small (at $\eta = \infty$, e.g., the value of the scaling parameter must exceed $\alpha = 28.47$ or $\alpha = 0.04$, respectively, for the two sets of fixed points).

(iii) For $\eta \gtrsim 1.6$ one has, in addition, a limit cycle which attracts most trajectories out of the sample we used in our search for the attractors. The projection of this limit cycle onto the (Φ_1, Φ_2)-plane is centred around $\Phi_1 = \Phi_2 = \pi$ and $\Phi_3(t)$ increases monotonically in steps of width π, varying with the same period as do $\Phi_1(t)$ and $\Phi_2(t)$. Therefore one finds a closed curve in the coordinates $(\Phi_1, \Phi_2, \sin\Phi_3)$, cf figure 3. It is easy to understand this behaviour qualitatively by expanding the equations of motion around $\sin\Phi_{i=1,2} = \pi$. In a certain sense this is typical 'Rössler behaviour'†. Therefore, we refer to it here as the 'generic' limit cycle. Below $\eta = 1.6$ period doubling sets in and the attractor turns chaotic—cf figure 4—before it vanishes near $\eta \approx 1.53$.

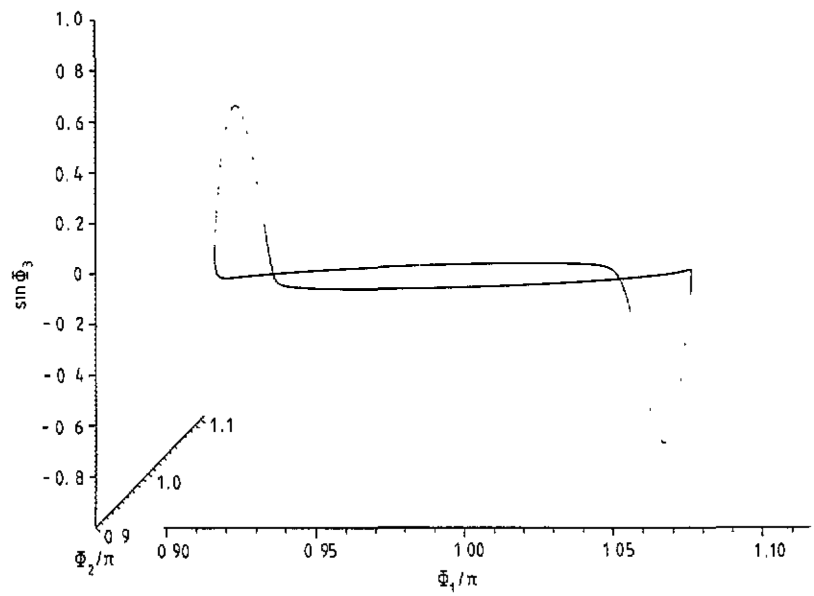

Figure 2. The limit cycle near the origin of the 'Rössler torus' beyond the second period-doubling transition; $\eta = 160$.

† Rössler characterizes the principle underlying his system (3.15)—and others generating 'spiral-type' chaos—as follows: 'combining a two-variable oscillator (in this case x and y) with a switching-type subsystem (z) in such a way that the latter is being switched by the first while the flow of the first is dependent on the switching state of the latter' [13].

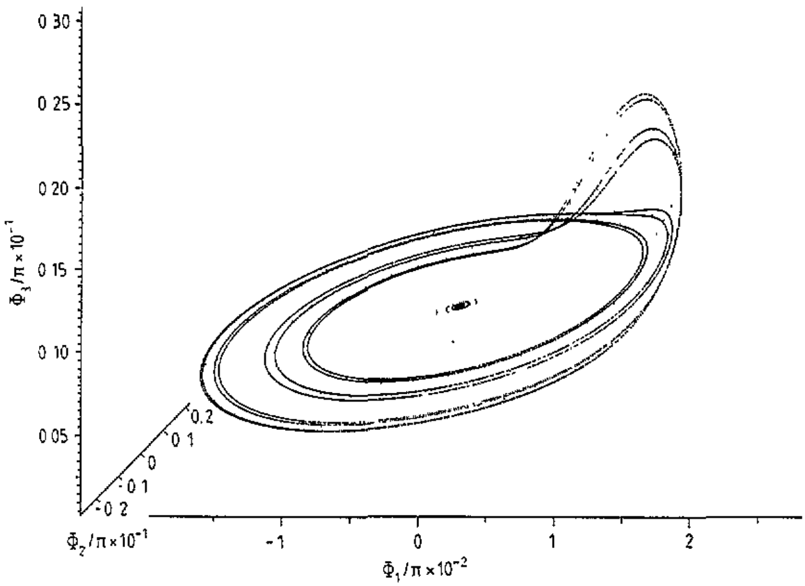

Figure 3. The 'generic' limit cycle on the 'Rössler torus' centred around $(\Phi_1, \Phi_2) = (\pi, \pi)$ in the (Φ_1, Φ_2)-plane; Φ_3 is monotonically increasing. $\eta = \infty$.

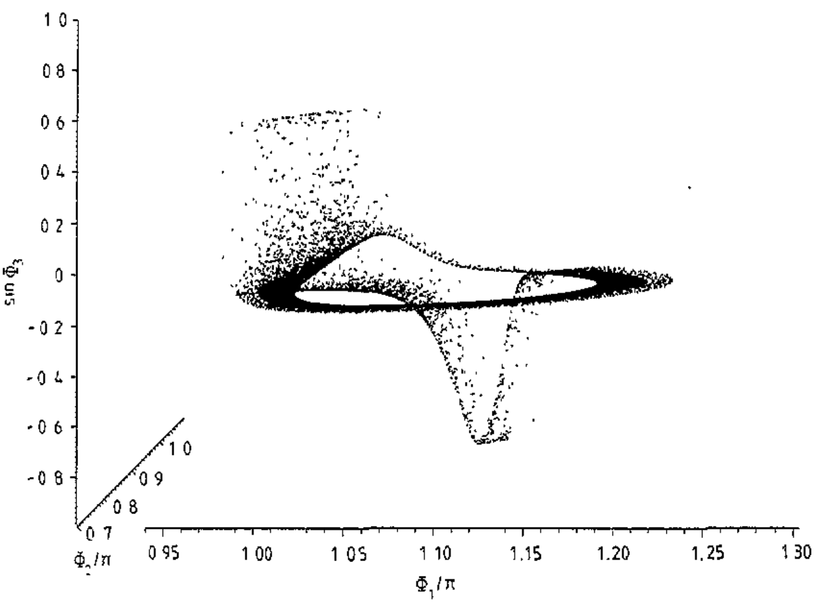

Figure 4. The 'generic' periodic attractor on the 'Rössler torus' has turned chaotic; $\eta = 1.536$.

Notwithstanding some differences in detail, the overall picture of the motion on the isolated strange 'Lorenz-torus'is very similar to this behaviour on the isolated strange 'Rössler torus' [6] (cf the footnote in section 5).

4. Non-isolated non-regular Hamiltonian tori

As we have seen in section 1 non-regular tori need not be isolated in phase space. In the following section we demonstrate that the attractors of (quasi-)periodically driven systems may occur on non-isolated non-regular tori forming invariant planar areas in phase space. In section 4.2 we show that the finite dimension n of the invariant manifold M_n in action space formed by the non-regular tori leads to important consequences for the flow on the tori: the number of vanishing Lyapunov exponents is constrained to be $\geqslant n$, and periodic motion may be impossible if $n \geqslant 2$.

4.1. Attractors of (quasi-)periodically driven systems on non-regular tori

Since the matrix $\partial F/\partial I_*$ in the equations of motion (1.5) has rank $m = N - n$ there always exists a linear canonical transformation such that the transformed equations of motion have a same simple structure: n of these equations are trivially integrable, and their solutions depend linearly on time. Inserting these solutions into the other equations we are left with $m = N - n$ non-trivial equations explicitly depending on time. In general an appropriate rotation of the coordinate axis is necessary in order to reduce the equations of motion (1.5) to this simple form and the transformed coordinates need not be angles (cf the detailed discussion in [6]). Here we restrict ourselves to the simplest case where the system of equations of motion is separated into n trivial equations and $m = N - n$ others without further transformation. As an example let us apply the procedure of section 3.1 to the periodically driven Duffing oscillator

$$\ddot{x} + \mu\dot{x} + k_{\mathrm{H}}\omega^2 x + \kappa x^3 = a_1\cos(\omega_1 t) \tag{4.1}$$

where $k_{\mathrm{H}} = 1$ or $k_{\mathrm{H}} = 0$ (in the latter case one has a purely anharmonic oscillator). Substituting $x_1 \equiv x$ and $x_2 \equiv \dot{x}_1/\omega$ one arrives at a non-autonomous system of two first-order differential equations. Proceeding as outlined in section 3.1, and subsequently extending the phase space in order to eliminate the explicit time dependence by substituting $\Phi_3 \equiv \omega_1 t$, one gets the following equations of motion

$$\begin{aligned}
\dot{\Phi}_1 &= \frac{\omega_{0,1}(I_*)}{\eta} + \omega\sin\Phi_2 \\
\dot{\Phi}_2 &= \frac{\omega_{0,2}(I_*)}{\eta} - \mu\sin\Phi_2 - k_{\mathrm{H}}\omega\sin\Phi_1 - \frac{\kappa\alpha^2}{\omega}\sin^3\Phi_1 + \frac{a_1}{\omega\alpha}\cos\Phi_3 \\
\dot{\Phi}_3 &= \frac{\omega_1}{\eta}
\end{aligned} \tag{4.2}$$

for action values I_* on the straight line $M_1 = \{I_* \mid I_{*,i} = I_{0,i}, i = 1, 2\}$ (therefore, $n = 1$). Thus, the procedure yields invariant 3-tori forming a four-dimensional invariant manifold in the six-dimensional phase space.

For sufficiently large values of the scaling parameter α we find the well known attractors of the periodically driven Duffing oscillator [14, 15] near $\Phi_1 = \Phi_2 = 0$ if $\omega_{0,1} = \omega_{0,2} = 0$ and $\eta = 1$ (note that the scaling increases the nonlinearity but decreases the driving force). These attractors are periodic or chaotic ones, depending on the value of the driving amplitude a_1. Figure 5 shows such a chaotic attractor (the time step chosen is not small relative to the average time of revolution on the

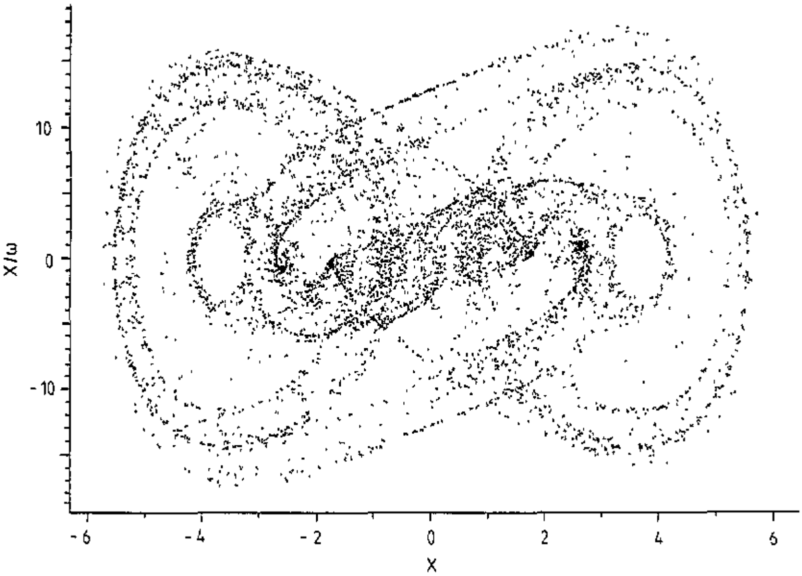

Figure 5. A strange attractor of the periodically driven Duffing oscillator found near $\Phi_1 = \Phi_2 = 0$ on a 'Duffing 3-torus'. Lyapunov exponents: $\lambda_1 = 0.097$, $\lambda_2 = 0$, $\lambda_3 = -0.297$. Parameters: $\mu = 0.2$, $k_H = 1$, $\kappa = 1$, $\omega = \omega_1 = 1$, $a_1 = 55$, $\eta = 1$ and $\alpha = 10^{10}$. Time step $\Delta t = 0.5$, $T/\Delta t = 20\,000$ points displayed.

attractor). For the Lyapunov exponents given in the legend one has $\lambda_1+\lambda_2+\lambda_3 = -\mu$ as required for a system with a constant value of the Jacobian (cf [20, ch 7.1]).

Equations (4.2) describe the motion of an electron—which has the appropriate momentum—with two spatial degrees of freedom (x and y) in a periodically time-dependent field. However, if one identifies

$$\Phi_3 \equiv 2\pi\frac{z}{z_0} \qquad \text{and} \qquad \omega_1 \equiv \omega_{0,3}(I_*) \tag{4.3}$$

cf the last paragraph of section 2—these equations describe the motion of an electron with three degrees of freedom in a *stationary* field. In this case the action variable I_3 has a direct physical interpretation, namely $I_3 \sim \dot{z} =$ constant (since $A_z = 0$). Thus we see that even in the simplest case where the equations of motion are separated into trivial and non-trivial ones from the outset (without further transformation) they may be autonomous ones, rather than being only formally autonomous as our original equation (4.2).

As another example we apply our standard procedure to quasiperiodically driven Duffing oscillators, i.e. we replace the driving force in (4.1) by a sum $\sum_{i=1}^{n} a_i \cos(\omega_i t)$ containing two or more (generically) incommensurate driving frequencies ω_i. We thus arrive at a system of equations of motion which is a trivial extension of the system (4.2). Clearly, periodic motion, and thus the occurrence of periodic attractors, is excluded in the generic case of incommensurate driving frequencies. As the number m of non-trivial equations is fixed ($m = 2$ in the Duffing case) the equations of motion describe the motion of an electron with two spatial degrees of freedom in quasiperiodically time-dependent electromagnetic fields. However, if we insert (4.3) and let $n = 2$, we find that the equations also characterize the motion of an electron with three spatial degrees of freedom in *periodically* time-dependent electromagnetic fields. Treating 'time' and energy again as canonical variables in an enlarged phase space the trajectories of the electron are situated on invariant 4-tori forming a six-dimensional invariant plane in the eight-dimensional phase space. We study a purely anharmonic Duffing oscillator, i.e. $k_{\rm H} = 0$, and set $\alpha = 1$ (no scaling). Thus we do *not* expect to find the attractors of the original quasiperiodically driven Duffing oscillator oscillator near $\Phi_1 = \Phi_2 = 0$ for $\omega_{0,1} = \omega_{0,2} = 0$ and $\eta = 1$. At small driving amplitudes $a_{i=1,2}$ we find there aperiodic attractors with a Lyapunov spectrum of the form $(0, 0, -, -)$. The motion on one of these regular aperiodic attractors is shown in figures 6 and 7. Whereas the latter contains a Poincaré plot for a fixed value of Φ_4 the former displays a projection into the (Φ_1, Φ_2) plane (the time step chosen in this case is again not small relative to the average time of revolution on the attractor). One should note that the *details* of this picture change markedly if the time step is only slightly varied whereas the general impression of regularity does not. Reducing as it does the dimension by one, the fact that the Poincaré section of the attractor yields a simple curve proves that the attractor is really a—already somewhat distorted—2-torus in the four-dimensional space of the angles. If one enhances the driving the torus 'breaks up', as is clear in figure 8 (a projection into the (Φ_1, Φ_2) plane gives a more or less uniform distribution of points which is slightly more extended than the one in figure 6).

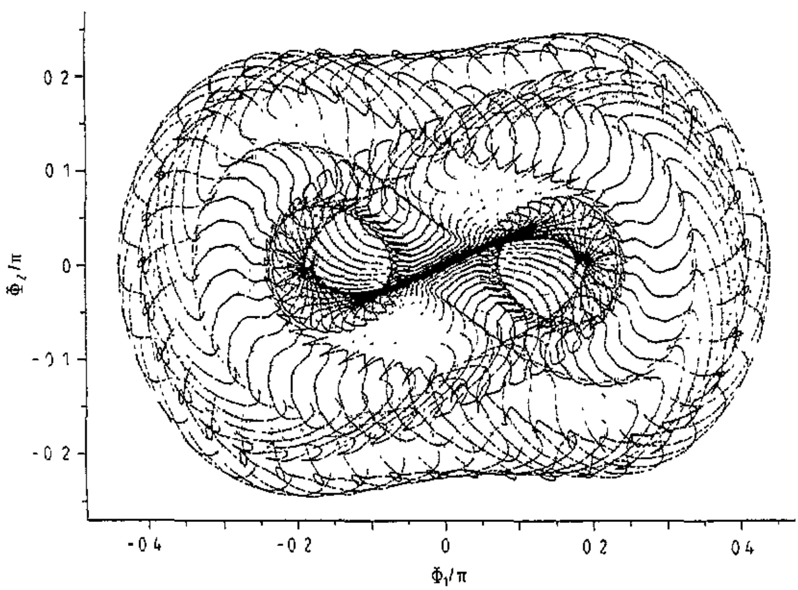

Figure 6. Projection of a regular non-periodic attractor on a 'Duffing 4-torus' into the (Φ_1, Φ_2)-plane. Lyapunov-exponents: $\lambda_1 = \lambda_2 = 0$, $\lambda_3 = -0.04$, $\lambda_4 = -0.06$. Parameters: $\mu = 0.1$, $k_H = 0$, $\kappa = 1$, $\omega = 1$, $\omega_1 = \sigma_g$, $\omega_2 = \sigma_g^2$, $a_1 = 0.1$, $a_2 = 0.2$ and $\eta = \alpha = 1$. Time step $\Delta t = 0.5$, $T/\Delta t = 50\,000$ points displayed.

4.2. *Consequences of the finite dimension of the invariant manifold*

In Hamiltonian systems of the form (1.4) non-regular N-tori form invariant areas with dimensions

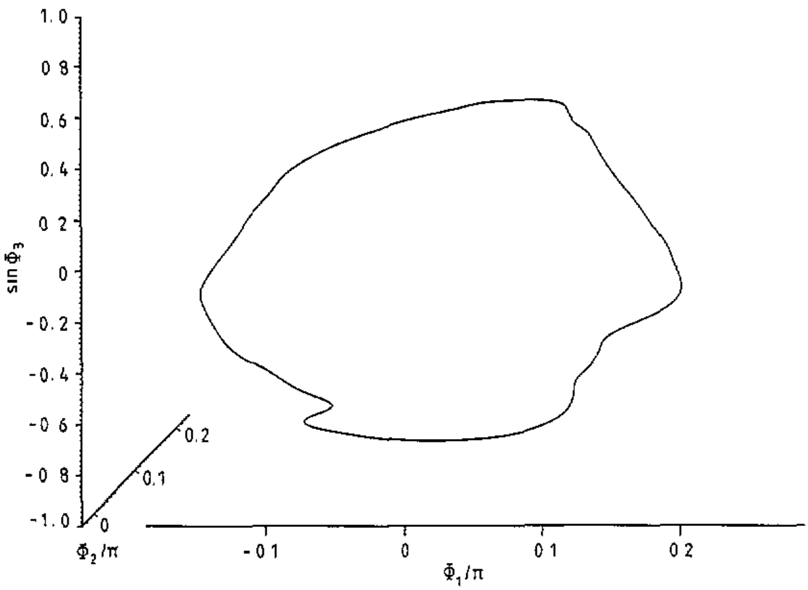

Figure 7. Poincaré section of the attractor shown in figure 6. The value of Φ_4 is fixed ($\Rightarrow$ time step $\Delta t = 2\pi/\omega_2$).

$$D_n = N + n \tag{4.4}$$

ranging from $N+1$ up to $2N-1$. And yet, these tori have clearly measure zero in the $2N$-dimensional phase space. This is in contrast to KAM tori which fill a part of finite measure in the phase space of near-integrable Hamiltonian systems having N degrees of freedom. It is interesting to compare the dimension D_n (4.4) to the dimension $D_{\rm reg}$ of a manifold of KAM tori having the same normalized frequency vector $\tilde{\Omega} = \Omega / \mid \Omega \mid$. Since there are N free angle variables on these tori which in turn exist in an energy interval one has

$$D_{\rm reg} = N + 1. \tag{4.5}$$

Therefore, non-regular tori can form barriers† in Hamiltonian systems of the form (1.4) with *any* number of degrees of freedom whereas KAM tori cannot form barriers in near-integrable systems with more than *two* degrees of freedom.

Important conclusions can be drawn from the fact that n is the number of relevant frequencies whereas $m = N - m$ is the number of relevant differential equations: n of the Lyapunov exponents characterizing the motion vanish whereas the m remaining ones need not. Chaotic attractors may thus exist if $m > 1$. This excludes barrier tori in Hamiltonian systems of the form (1.4). The dimension of the attractors on barrier tori may still be fractal, i.e. one may find *strange non-chaotic attractors* on barrier tori if $N \geqslant 3$. Such attractors have been found among the solutions of one first-order differential equation containing quasiperiodic driving terms ($n = 2$) [16].

† An invariant $(2N-1)$-dimensional manifold is an (insurmountable) *barrier* for the flow in the $2N$-dimensional phase space if it contains the surface of a $2N$-dimensional manifold. Then the flow is everywhere tangential to that surface, and thus trajectories cannot cross it. Other invariant $(2N-1)$-dimensional manifolds are also barriers (but not insurmountable ones).

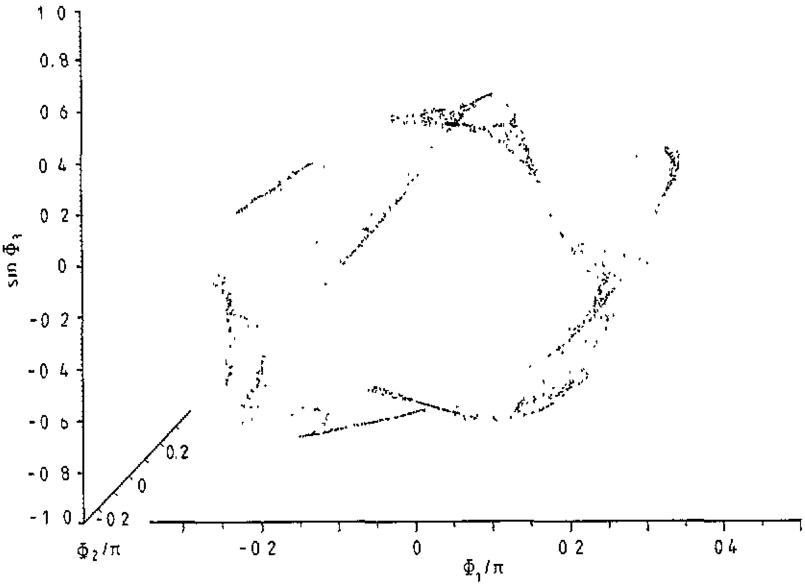

Figure 8. Transition to a chaotic attractor on a 'Duffing 4-torus': Poincaré section of the attractor shown in the two preceding figures, but now at anhanced driving (all parameters unchanged except for $a_1 = 0.1625$). Again, the value of Φ_4 is fixed. Non-vanishing Lyapunov exponents: $\lambda_1 = 0.01$, $\lambda_4 = -0.09$. According to the well known Kaplan–Yorke conjecture [22] this implies that the information dimension of the attractor is $d_f \approx 3.1$, i.e. fractal.

Periodic motion becomes impossible if $n \geqslant 2$ and the frequencies $\omega_{i=1,\dots,n}$ constituting the right-hand sides of the n trivial equations are incommensurate. Thus, periodic attractors, i.e. limit cycles, cannot exist on these tori if this commensurability condition is not fulfilled. Of course the attractors may still be regular ones, cf the example of the 'Duffing 4-tori' in section 4.1 (especially figures 6 and 7).

5. Conclusions

We have investigated the motion on Hamiltonian tori which are not of KAM type. The flow on these invariant tori is—generically—dissipative and non-integrable. Therefore, attractors can occur on such *non-regular* tori which may be strange ones in systems with three or more degrees of freedom. On the other hand, non-regular tori may be reduced to KAM tori if the perturbation is small enough (the measure of the set of points on the η-axis where such a reduction is possible is finite and tends to 1 with $\eta \to 0$). Thus, we find a new 'chaos scenario': KAM tori which transform into non-regular ones rather than breaking up when the perturbation becomes strong.

Non-regular tori may be isolated in phase space but need not be. They form invariant areas with dimensions ranging from N up to $2N-1$. Thus, barriers consisting of such invariant tori may occur in the phase space of Hamiltonian systems with any number N of degrees of freedom whereas KAM tori cannot form barriers for $N > 2$. The motion on such non-regular barrier tori is always regular, though. Still, one may find strange non-chaotic attractors there. On non-isolated ones which are not part of a barrier chaotic (strange) attractors may occur. A simple procedure has been used which allows to specify Hamiltonian systems with non-regular tori containing well known (strange) attractors—and structurally identical repellers—such as the Rössler attractor or the attractors of the driven Duffing oscillator. Attractors of autonomous dissipative systems are found on isolated non-regular tori whereas those of (quasi-)periodically driven systems occur on non-isolated tori. Furthermore, limit cycles have been observed which transform via period-doubling sequences into chaotic attractors when the perturbation strength is varied†. On non-regular tori related to quasiperiodically forced systems regular but aperiodic attractors replace the limit cycles. Fixed points, and hence point attractors, (generically) only occur on isolated non-regular tori. Although we did not give an example it should be mentioned that 'transient repellers' [22] may exist on non-regular tori as well.

In this paper we present a model of a Hamiltonian system containing such non-regular tori, isolated ones as well as non-isolated ones: an electron moving in certain electromagnetic fields which are periodic in space. Even if these fields are stationary the motion of the electron on a non-regular torus may correspond to that of a *periodically driven* system, e.g. the Duffing oscillator (cf section 4.1). It should be noted, though, that in our model non-isolated tori form always planar invariant areas in phase space whereas in general such invariant areas may be non-planar. Furthermore, we did not attempt to check whether the space-periodic charge and current densities required for building up the electromagnetic fields can be easily generated in an experiment.

The study of the motion on non-isolated non-regular tori has been restricted to the region near the origin (with respect to the 'non-trivial' components) whereas in the case of isolated tori we have concentrated on the investigation of the motion in systems with moderate and large perturbations ($\eta \gtrsim 1$). This is justified by the fact that the flow on tori with (at least) one monotonically advancing angle variable has already been considered elsewhere [9–12] by exploiting the then possible reduction in the continuous dynamics to the study of discrete maps (cf section 1).

Acknowledgment

One of us (HL) wants to thank the International Relations Office, KfK, Karlsruhe for partial support (project number X231.3).

References

[1] Kolmogorov A N 1954 *Dokl. Akad. Nauk USSR* **98** 527 (Engl. transl. Bao Lin H (ed) 1990 *Chaos II* (Singapore:World Scientific) p 107)
[2] Arnol'd V I 1963 *Russ. Math. Surv.* **18** 9
[3] Moser J 1967 *Math. Ann.* **169** 136; 1973 *Stable and Random Motions* (Princeton, NJ: Princeton University Press)
[4] Arnol'd V I 1961 *Izv. Akad. Nauk USSR, Ser. Mat.* **25** 21 (Engl. transl. 1965 *AMS. Transl. Ser.* 2 **46** 213)
[5] Herman M R 1979 *Pub. Math. I.H.E.S.* **49** 5
[6] von Kempis A 1992 *Thesis* Universität Duisburg Jül-Report (Berichte des Forschungszentrums Jülich)

† This occurs also on non-isolated strange tori [6]. An intermittent transistion from a periodic to a chaotic attractor has been observed on an isolated strange 'Lorenz torus' (cf section 3.3).

[7] Salat A 1988 *Phys. Scr.* **38** 17; 1986 *IPP Report* 6/257
[8] Lorenz E N 1963 *J. Atmos. Sci.* **20** 130
[9] Grebogi C, Ott E and Yorke J A 1983 *Phys. Rev. Lett.* **51** 339; 1985 *Physica* **15D** 354
[10] Battelino P M 1988 *Phys. Rev.* A **38** 1495
[11] Battelino P M, Grebogi C, Ott E and Yorke Y A 1989 *Physica* **39D** 299
[12] Baesens C, Guckenheimer J, Kim S and McKay R S 1991 *Physica* **49D** 387
[13] Rössler O E 1976 *Phys. Lett.* **57A** 397
[14] Ueda Y 1979 *J. Stat. Phys.* **20** 181
[15] Schmidt K 1986 *Diploma Thesis* Universität Frankfurt/Main unpublished
[16] Romeiras F J and Ott E 1987 *Phys. Rev.* A **35** 4404
Bondeson A, Ott E and Antonsen T M Jr *1985 Phys. Rev. Lett.* *55* *2103*
[17] Wolf A, Swift J B, Swinney H L and Vastano J A 1985 *Physica* **16D** 285
[18] Haken H 1983 *Phys. Lett.* **94A** 71
[19] Crutchfield J, Farmer D, Packard N, Shaw R, Jones G and Donnelly R J 1980 *Phys. Lett.* **76A** 1
[20] Lichtenberg A J and Lieberman M A 1983 *Regular and Stochastic Motion* (New York: Springer)
[21] Kaplan J L and Yorke J A 1979 *Lecture Notes in Mathematics 730* ed H O Peitgen and H O Walther (Berlin: Springer) p 228
[22] Tél T 1990 *Directions in Chaos III* ed Hao Bai-lin (Singapore: World Scientific) p 149